１７．Observation of L1-SAIF Signal in Australia
L1-SAIF 信号オーストラリア受信実験

University of New South Wales, Australia, ※Yong Li, Mazher Choudhury, Chris Rizos

1. Introduction

The QZSS (Quasi-Zenith Satellite System) L1-SAIF (Submeter-class Augmentation with Integrity Function) development is undertaken by ENRI (Electronic Navigation Research Institute, Japan), in order to provide wide area differential corrections to GPS uses with a target accuracy of 1m (horizontal). In addition to the messages which are fully compatible with SBAS (Space-Based Augmentation System), L1-SAIF includes extra definable messages.

To investigate potential use of L1-SAIF services in Australia, a collaboration project between UNSW and ENRI has been established. The L1-SAIF messages from QZSS and MSAS (MTSAT Satellite Augmentation System) were collected at two stations, in Sydney and Melbourne, during the project period, especially a continuous data collection experiment from September to November in 2014. As the first step of this investigation, the visibility of the QZSS and MSAS satellites in Australia is evaluated from the collected data. This study can provide a pattern of the real L1-SAIF signals in the Australian region – how often its visibility is, and what is its signal strength.

The magnitude of the ionospheric delay depends on a number of factors, such as the latitude of the receiver, the elevation of the satellite in view at the time of observation, the season, the time of day, and the level of solar activity. The ionospheric delay of signals from satellites overhead can be several tens of metres. The elevation angle to the satellite is quite significant since delay increases with lower elevations; being up to about five times greater near the horizon than overhead [1]. This is largely due to the longer signal path through the ionosphere. Paths to satellites closer to the horizon (at low elevations) have a slanting line through the ionosphere which of course is longer than a vertical path.

Provided that a MSAS or QZSS satellite is available to the MSAS/QZSS reference station network for tracking purposes, orbit and timing error corrections will be available for that satellite. Ionosphere corrections for that satellite are only available if the signal passes through the ionospheric map provided by MSAS or QZSS (at present the L1-SAIF ionospheric map covers the Japan and nearby region). As QZSS and MSAS satellites are visible in the northwestern portion of the sky in Australia, the L1-SAIF signals from QZSS and MSAS may travel through equatorial regions, which more likely happens when the satellite has a low elevation angle. This may create extra difficulty for the estimation of the ionospheric delay of L1-SAIF in Australian regions because of the phenomenon known as Equatorial Anomaly.

2. Experiment configuration

The Javad Alpha GNSS receivers were utilised in the tests in Sydney and Melbourne. The Leica AS10 antenna was used in Sydney, and Javad Delta receiver and GrAnt-G3T antenna were used in Melbourne. The Javad NetView program was used to configure the receivers and store the data onto the hard disk of the host computer via a serial port.

The antenna setups used in the experiments in Sydney and Melbourne are shown in Figures 1 and 2. As shown in Figure 1, there is a tall tree close to the antenna in the northwestern direction, which could partly attenuate low elevation signals from this direction.

The GNSS raw measurements were recorded in the binary format of the Javad protocol [2], which includes GPS, GLONASS, Galileo, QZSS, and MSAS measurements. The updating rate is configured as 1Hz.

Figure 1 Antenna setup at Sydney station

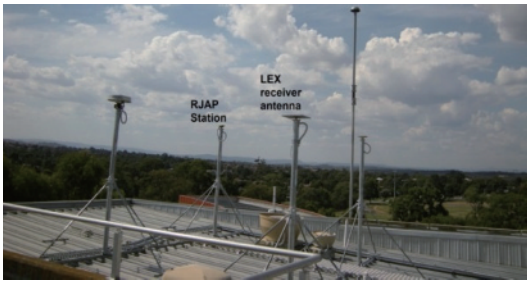

Figure 2 Antenna setup at Melbourne station

Three months of continuous data logging was conducted in Sydney and Melbourne at the same time during the period of 1 September – 30 November 2014.

The RTKIB version 2.4.3 software was used to process the RINEX files that were converted from the data recorded by the Javad receivers. The TEQC software was used to analyse the ionosphere of L1-SAIF signals. The results below are visualised elevation of QZSS, signal level of L1_SAIF, and code-phase multipath of L1-SAIF.

3. Experiment results

The JPS data were recorded in files every day during the period Sep – Nov 2014. The JPS files were converted into RINEX3.02 for visibility, signal level, and multipath analysis. The JPS files were also converted into RINEX2.10 for ionosphere analysis. The first day of the month during the experimental period is chosen for the analysis. The result of 1st of September is presented in this paper. More results can be found in the project report [3].

3.1 L1-SAIF visibility and signal level analysis

The SNR, code-phase multipath, and elevation are plotted against time by RTKLIB. The plots of the data observed at Sydney station on 1st of September are shown in Figures 3-6.

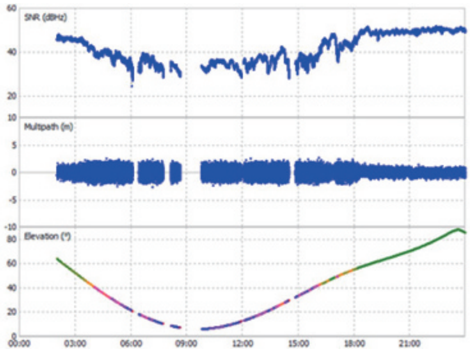

Figure 3 Visibility of L1-SAIF of QZS on 2014-09-01 at Sydney station

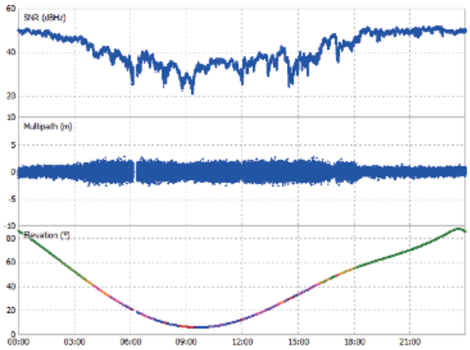

Figure 4 Visibility of L1C of QZS on 2014-09-01 at Sydney station

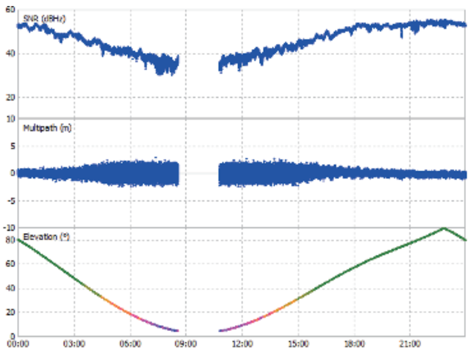

Figure 5 Visibility of L1-SAIF of QZS on 2014-09-01 at Melbourne station

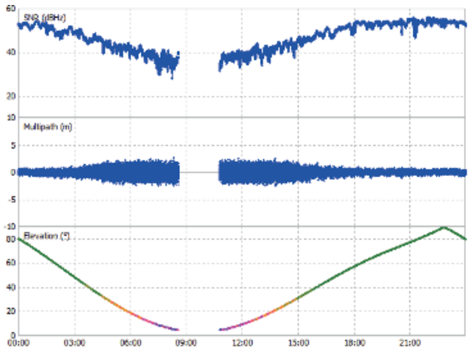

Figure 6 Visibility of L1C of QZS on 2014-09-01 at Melbourne station

For an easy view of the visibility and signal level of the L1-SAIF data, the same plot of L1C data is shown together with the plot of L1-SAIF, see Figures 4 and 6.

From Figures 3 and 4 it can be seen that the SNR >40dB during the time QZS at high elevation at the Sydney station (because of the tree near the antenna). However, from Figures 5 and 6 the L1-SAIF signal is strong of SNR > 40dB most of the time at the Melbourne station because the antenna has an unobstructed sky view

From Figures 3 and 4 it can be seen that the SNR and MP (code-phase multipath) of L1-SAIF and L1C are similar. They have the same trend – the lower elevation the smaller SNR, meanwhile the lower SNR the bigger MP. This is as expected from theoretical prediction. The same results were obtained for all other days at both the Sydney and Melbourne stations [3]. There were multiple instances of data gaps which can be observed from the figures. These gaps are largely due to missing observations in the RINEX files. At this stage the main reasons are found to be due to: (1) the low elevation of the QZS, this is clearly shown in Figures 3-6 in both Sydney and Melbourne tests; (2) the tree near the antenna at Sydney station blocked the low elevation signals from northwestern direction, see Figure 7.

The tree is about 3m away and has a tall of about 3~4m above the antenna, which makes a shadow of about 45deg low, which attenuates the QZS signals under elevation of 45deg. This is the main reasons that the data gaps in in Figure 3.

From Figures 3 and 4, it can be seen that L1-SAIF data suffered more interrupts than the L1C data at the Sydney station. From Figures 5 and 6, interrupts on L1-SAIF and L1C are similar, which were caused by QZS setting below the horizon, which lasted for about 2 hours [3].

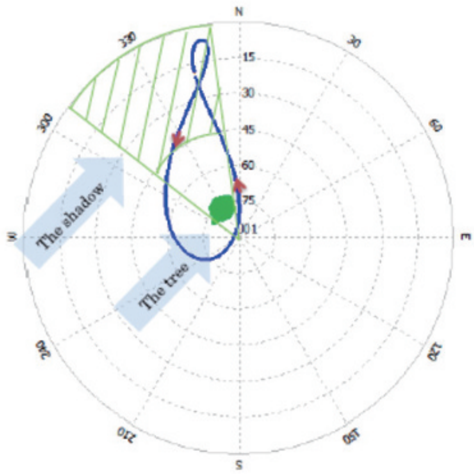

Figure 7 The signals attenuation under the tree shadow

3.2 L1-SAIF ionosphere analysis

The ionospheric delay can be derived from the combination of L1 and L2 carrier phase measurements [4], which is written as:

$$I_1 + \frac{1}{\alpha-1}[n_1\lambda_1 - n_2\lambda_2 + m_1 - m_2] = \frac{1}{\alpha-1}(L_1 - L_2) \quad (1)$$

$$I_2 + \frac{\alpha}{\alpha-1}[n_1\lambda_1 - n_2\lambda_2 + m_1 - m_2] = \frac{\alpha}{\alpha-1}(L_1 - L_2) \quad (2)$$

where I_1 and I_2 are the ionospheric delay on the L1 and L2 signal frequencies; λ_1 and λ_2 are the wavelengths of L1 and L2; n_1 and n_2 are the integer ambiguities on L1 and L2; m_1 and m_2 are the multipath on L1 and L2. The factor $\alpha = f_1^2/f_2^2$, where $f_1 = 1575.42$MHz and $f_2 = 1227.60$MHz are the frequencies of L1 and L2 respectively.

The time-rate of change of ionospheric delay is defined as [4]:

$$IOD_2 = \frac{\alpha}{\alpha-1}\left[(L_1 - L_2)_j - (L_1 - L_2)_{j-1}\right]/(t_j - t_{j-1}) \quad (3)$$

where IOD_2 is the change rate of ionospheric delay of L2 over the period of time (t_{j-1}, t_j).

In fact, the ionospheric delay observable calculated by TEQC is actually obtained by (as shown by Appendix B [3]):

$$IONO_j = IONO_{j-1} + IOD_2\ (t_j - t_{j-1}) \qquad (4)$$

where $IONO_j$ is the ionospheric delay observable at epoch j.

It can be seen that the ionospheric delay observable is the accumulation of the IOD2. This is the reason why, in Figures 8 and 9, the ionospheric delay observables change from positive to negative values along with time of a day.

As shown in Figures 8 and 9, the ionospheric delay of QZS varies rapidly around 5:00 (GPST) that is the noon of Australian Eastern Time (AET), which means the ionosphere is relatively active during this period of time. However the ionospheric delay does not change so much around 19:00 (GPST, that is the early morning 3am in AET), indicating that the ionosphere is calm during this period of time.

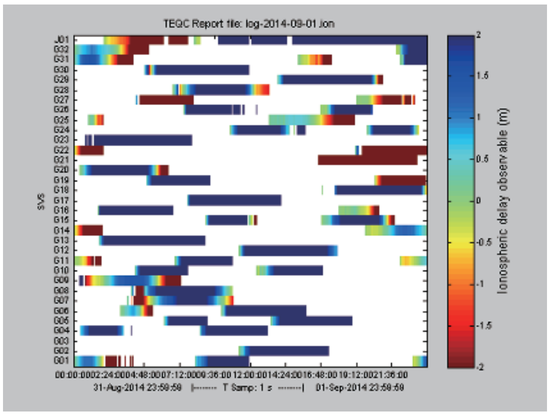

Figure 8 Ionospheric delay of L1-SAIF from QZS on Day 2014-09-01 at Sydney station

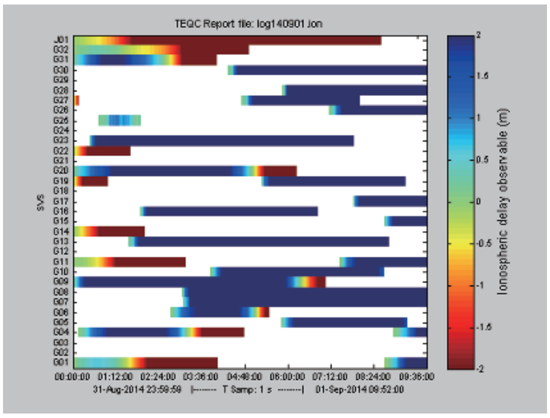

Figure 9 Ionospheric delay of L1-SAIF from QZS on Day 2014-09-01 at Melbourne station

4. Concluding remarks

The 3-month continuous data collection campaign was conducted during September to November 2014, in both Sydney and Melbourne. The data have been analysed to address on the visibility and signal strength of L1-SAIF signal in Australia. Some concluding remarks can be drawn:

(1) The L1-SAIF signals can be received for most of the day, except (a) the QZS setting below the horizon; (b) the tree near the antenna at the Sydney station blocked low elevation signals from the northwestern direction.

(2) The L1-SAIF signal is strong, with SNR > 40dB for most of the time at the Melbourne station with an unobstructed sky view. SNR >40dB during the time QZS was at high elevation was also observed at the Sydney station.

(3) The SNR and multipath of L1-SAIF and L1C are similar. They have the same trend – the lower the elevation the smaller the SNR, and the lower the SNR the larger the MP.

(4) The ionospheric delay of QZS can reflect ionospheric activity, for example the ionospheric was clam in early morning of AET.

References

[1] UNAVCO, “Teqc Tutorial – Basics of Teqc Use and Teqc Products”, June 2014.

[2] Javad, “GNSS Receiver External Interface Specification”, Reflects firmware ver 3.4.6, Rev Oct 2012.

[3] Y. Li, M. Choudhury, C. Rizos, “ Study on Expansion of GNSS Wide Area Augmentation Service to the Asia Region”, technical report on the UNSW-ENRI L1-SAIF project, April 2015.

[4] L.H. Estey and C. M. Meertens, “TEQC: The Multi-Purpose Toolkit for GPS/GLONASS Data”, GPS Solutions, Vol.3, No.1, pp.42-49, 1999.